CSIRO PUBLISHING
Soil Research, 2013, **51**, 262–277
http://dx.doi.org/10.1071/SR12347

Development of class pedotransfer functions for integrating water retention properties into Portuguese soil maps

T. B. Ramos[A,D], *M. C. Gonçalves*[A,B], *D. Brito*[C], *J. C. Martins*[B], *and L. S. Pereira*[A]

[A]CEER, Institute of Agronomy, Technical University of Lisbon, Tapada da Ajuda, 1349-017 Lisbon, Portugal.
[B]INIAV, National Institute of Agronomic and Veterinarian Research, Av. República, 2784-505 Oeiras, Portugal.
[C]MARETEC, Technical Superior Institute, Technical University of Lisbon, Av. Rovisco Pais 1, 1049-001 Lisboa, Portugal.
[D]Corresponding author. Email: tiago_ramos@netcabo.pt

Abstract. Hydrological modellers have recently been challenged to improve watershed models by better integrating soil information into model applications. Reliable soil hydraulic information is thus necessary for better describing the water balance components at the catchment scale. Frequently, that information does not exist. This study presents a set of class-pedotransfer functions (PTFs) for estimating the water retention properties of Portuguese soils. The class-PTFs were established from a dataset containing 697 soil horizons/layers, by averaging values of total porosity and volumetric water contents at –0.25, –1, –3.2, –6.3, –10, –33, –100, –250, and –1500 kPa matric potentials after grouping data by soil texture class, soil horizon, and bulk density. Fitted retention curves using the van Genuchten model were also obtained for every class-PTF. The root mean square error varied between 0.039 and 0.057 cm^3/cm^3, with smaller values found when using the 12 texture classes of the International Soil Science Society (ISSS) system rather than the five texture classes of FAO, and when bulk density was also considered. The class-PTFs were then integrated into Portuguese soil maps and its usage was demonstrated by deriving maps of available water capacity to be used for modelling the water balance in a small catchment area with the SWAT model. The model successfully simulated the reservoir inflow when using the derived maps, but the results did not vary much whether using coarser or finer description of the catchment soils. Nonetheless, the class-PTFs contributed to a better soil characterisation than when using coarse-scaled information. The approach followed here was simple, inexpensive, and feasible for modellers with few resources but interested in considering the spatial variability of soil retention properties at large scales and in advancing hydrologic modelling in Portugal.

Additional keywords: bulk density, soil grouping, soil horizons, soil mapping units, texture classes.

Received 25 November 2012, accepted 24 June 2013, published online 2 September 2013

Introduction

Recently, watershed modelling has emerged as one of the most important assessment tools in watershed planning and management. Nonetheless, hydrological modellers have been challenged to improve watershed models by better integrating soil information into model applications (Lin *et al.* 2006; Bouma *et al.* 2011). Soil type is a major factor influencing soil evaporation, crop evapotranspiration, crop nutrition, recharge to groundwater, and soil erosion. In addition, soil physical and chemical properties present inherent spatial and temporal variability within the catchment scale. However, in many model applications, soils have been considered simplistically, frequently as homogeneous and isotropic, simplifying important hydrologic processes occurring at the catchment level (Bouma *et al.* 2011). As a result, the classic calibration of watershed models, in which a few discharge gauges near the outlet of a catchment are used to compare measured and simulated discharges, has been criticised because it does not assure that other processes such as evapotranspiration, crop growth, and groundwater recharge are correctly represented in the catchment area (Lin *et al.* 2006; Bouma *et al.* 2011).

Hydrological modellers generally have no alternative to these simplistic representations of field soils, because detailed and reliable soil information is rare in most regions of the world. Hydropedology, an emerging interdisciplinary field merging soil science and hydrology, intends to overcome such limitations in watershed modelling by better addressing the intimate relationships linking soil, landscape, and hydrology (Lin 2003, 2010; Bouma 2006; Lin *et al.* 2006; Pachepsky *et al.* 2006; Bouma *et al.* 2011). Of particular interest to this study is the bridging of data gaps between soil survey databases and soil hydraulic information needed in simulation models. Classical methods for direct measurement of soil hydraulic properties (Dane and Topp 2002) are known to be costly, time-consuming, and impractical for large-scale applications in which many

samples are required to quantify the spatial and temporal variability of those properties. Remote-sensing techniques may eventually overcome those limitations and then be used to derive effective soil hydraulic properties at a much larger scale (Weihermüller *et al.* 2007; Steenpass *et al.* 2010; Jana and Mohanty 2012). However, further advancement in the research on these techniques is needed, as remote-sensing signals are usually sensitive only to a very limited surface depth and are unable to characterise the soil profile at the greater depths required in hydrological modelling. Hence, pedotransfer functions (PTFs), which relate soil hydraulic properties to basic soil physical and chemical properties usually available from soil survey studies (Bouma 1989; Vereecken *et al.* 1989; McBratney *et al.* 2002; Pachepsky and Rawls 2004), may still be the best approach when characterising soil hydraulic properties at large scales.

Soil survey studies can provide important information to improve hydrological modelling, especially soil maps, which are a common way to portray soil heterogeneity and to describe structural patterns across the landscape (Lin 2003, 2010). However, that information alone may not be sufficient, as soil hydraulic properties show spatial variability even within the same mapping unit (Wösten *et al.* 2001). Therefore, information obtained from soil survey studies should most likely be first used to derive a set of pedotransfer rules for each soil profile, which then could be used to integrate estimates of hydrological data and the associated uncertainty.

That strategy was the primary motivation in this study in which class-PTFs were developed as tools for assimilating soil hydraulic information into Portuguese soil maps. Class-PTFs provide class-average water contents at specific pressure heads or one average water-retention curve for every textural class. They are usually obtained from the arithmetic mean (e.g. Bruand *et al.* 2003; Al Majou *et al.* 2008*a*, 2008*b*), geometric mean (Wösten *et al.* 1995, 1999), and the statistical distribution of the dataset (Baker 2008). Hence, class-PTFs are considered the simplest approach for presenting reliable soil hydraulic information to hydrological modellers, as the models require only very basic soil data and are well suited for predicting water retention properties at regional or national scales (Wösten *et al.* 1995, 1999; Nemes *et al.* 2003; Al Majou *et al.* 2008*b*).

The simplicity of the data inputs of class-PTFs when compared with other more sophisticated PTFs (Gonçalves *et al.* 1997; Wösten *et al.* 1999; Schaap *et al.* 2001) also makes them ideal tools to overcome some of the constraints in the Portuguese soil survey database (Madeira *et al.* 2004; Gonçalves *et al.* 2005) if that information is to be used in modern hydrological modelling studies. Some of these constraints are: (*i*) different soil classification systems were used in the available soil maps, thus making basic soil properties such as soil texture classes the easiest link available among the different maps; (*ii*) soil maps within a single catchment area may show different levels of detail as a result of the scales used for mapping soils in different regions of the country; (*iii*) the coordinates of the representative soil profiles were never released, with only a broad location being given; and (*iv*) the information on soil hydraulic properties is limited to a few specific retention points (normally, the wilting point and field capacity), with most of the data being obsolete because they were determined on disturbed soil samples.

Consequently, most watershed modelling studies performed in Portugal have struggled to find reliable soil information for characterising field soils in their model applications (e.g. Nunes *et al.* 2006; Duarte *et al.* 2008; Yevenes and Mannaerts 2011). Some of these studies were able to proceed with a simplistic characterisation of soil hydraulic properties by analysing a few soil profiles in the studied areas. However, many others used data from Cardoso (1965), which are far from adequate in modern hydrological studies, or applied 'external' PTFs that have not been validated for Portuguese soils, sometimes not even accounting for the differences in the particle limits between the existing data and the requirements of the PTFs.

This study presents a set of class-PTFs developed from a currently underused database of Portuguese soil hydraulic properties (Gonçalves *et al.* 2011). The main purpose is thus to make the data available for watershed modellers, irrigation managers, and others, because data are more valuable when used by technicians, policy makers and scientists, including those interested in advancing hydrological modelling (Lin *et al*. 2006). The specific objectives of the study were to develop class-PTFs for integrating soil-water retention properties into Portuguese soil maps. Class-PTFs were derived for estimating water retention at 10 different values of matric potential, with soil texture classes, soil horizon, and bulk density being used as ancillary variables. Then, the effectiveness of the class-PTFs in simulations of a catchment water balance was assessed with the Soil and Water Assessment Tool (SWAT; Neitsch *et al.* 2011).

Materials and methods

The dataset

The class-PTFs were developed from data available in the PROPSOLO soil database (Gonçalves *et al.* 2011), which gathers all information on soil hydraulic and pedological properties from soil profiles obtained from research projects and academic studies performed at the Portuguese National Institute of Agronomic and Veterinarian Research (former Estação Agronómica Nacional). This database contains practically all of the existing knowledge on the soil hydraulic properties of Portuguese soils (with the exception of a few specific retention points found in soil survey studies).

The data extracted for this study included a set of 697 horizons/layers studied in 330 soil profiles in Portugal (Fig. 1) between 1977 and 2011. This dataset comprised 315 topsoil (0–30 cm depth) and 382 subsoil (>30 cm depth) horizons. The soil reference groups (FAO 1998) represented were Fluvisols (36.4%), Luvisols (29.4%), Vertisols (10.3%), Cambisols (8.5%), Calcisols (6.1%), Anthrosols (4.2%), Arenosols (1.5%), Podzols (0.9%), Regosols (0.9%), Ferralsols (0.6%), Leptosols (0.6%), and Planosols (0.6%). Table 1 presents the main physical and chemical properties of the 697 soil horizons/layers selected for the study. The particle size distribution was obtained using the pipette method for particles of diameter <2 μm (clay) and 20–2 μm (silt), and by sieving for particles 200–20 μm (fine sand) and 200–2000 μm (coarse sand). These textural classes follow the Portuguese classification system (Gomes and Silva 1962) and they are

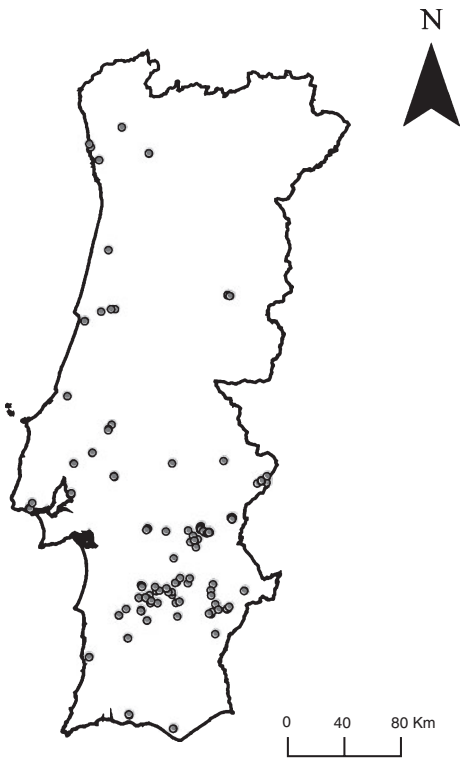

Fig. 1. Location of the 330 soil profiles in Portugal.

based on the International Soil Science Society (ISSS) particle limits (Atterberg scale). The organic carbon (OC) content was determined by the Walkley–Black method (Nelson and Sommers 1982). Dry bulk density (ρ_b) was obtained by drying volumetric soil samples (100 cm^3) at 105°C for 48 h. Total porosity (φ) was determined from the maximum holding capacity of 100-cm^3 undisturbed soil cores on a volumetric basis. Gravimetric water content was determined on undisturbed soil samples (100 cm^3) using suction tables at –0.25, –1, –3.2, –6.3, –10, and –33 kPa matric potentials (Romano *et al.* 2002) and the pressure plate apparatus at –33, –100, –250, and –1500 kPa matric potentials (Dane and Hopmans 2002). Then, the volumetric water content for each horizon/layer and each matric potential was computed from the gravimetric water contents and the bulk density of the corresponding horizon/layer. The volumetric water content at –33 kPa was obtained from only one method at the time (using suction tables with sand and kaolin until 2005 and using the pressure plate apparatus after 2006).

The missing values in the volumetric water content dataset were estimated by introducing values derived from the fitted van Genuchten model (1980):

$$S_e(h) = \frac{\theta(h) - \theta_r}{\theta_s - \theta_r} = \frac{1}{\left(1 + |\alpha h|^{\eta}\right)^{1-1/\eta}} \qquad (1)$$

where S_e is the effective saturation; θ_r and θ_s are the residual and saturated water contents (L^3/L^3), respectively; α (1/L) and η (–) are empirical shape parameters; and h is the pressure head (L). This procedure introduced an error to the subsequent calculations and model evaluations resulting from the non-perfect fit of the fitted model to the experimental data (root

Table 1. Main physical and chemical characteristics of the 697 soil horizons
θ_i, Volumetric water contents measured at $-i$ kPa matric potentials

	Particle size distribution (%)				Organic carbon (g/kg)	Bulk density (g/cm^3)	Total porosity (cm^3/cm^3)	Volumetric water content (cm^3/cm^3)							
	2000–200 µm	200–20 µm	20–2 µm	<2 µm				$\theta_{0.25}$	θ_1	$\theta_{3.2}$	$\theta_{6.3}$	θ_{10}	θ_{33}	θ_{100}	θ_{250}	θ_{1500}
N	–	–	–	–	–	–	697	690	691	692	552	696	661	301	331	697
Mean	20.7	34.2	21.5	23.6	8.24	1.50	0.441	0.424	0.399	0.370	0.348	0.332	0.286	0.239	0.210	0.162
s.d.	17.6	15.4	12.2	14.8	5.02	0.18	0.074	0.075	0.076	0.080	0.085	0.088	0.090	0.086	0.083	0.080
Min.	0.1	0.7	0.9	0.1	0.01	0.91	0.250	0.231	0.192	0.114	0.049	0.036	0.029	0.008	0.009	0.006
Max.	94.6	73.6	68.1	63.3	25.10	1.90	0.659	0.635	0.624	0.607	0.590	0.574	0.536	0.474	0.449	0.407

mean square error (RMSE) = 0.014 cm^3/cm^3), in line with published results (e.g. Nemes and Rawls 2006). The errors were thus relatively small compared with the errors usually obtained using PTFs, and therefore, the fitted values were assumed as if they were measured. Table 1 presents the number of determinations of the water content at each matric potential in the original dataset. The number of missing values can be found by subtracting those numbers from the full set of data used in this study (697, where 23.2% of the retention curves were complete while 1.9% missed four or five values).

Development of class-PTFs

The class-PTFs were developed by averaging the values of total porosity (φ) and volumetric water contents (θ) at –0.25, –1, –3.2, –6.3, –10, –33, –100, –250, and –1500 kPa matric potentials after grouping the data using the following criteria: (*i*) the five textural classes of the FAO triangle adapted to the ISSS particle limits (Gomes and Silva 1980) and the 12 textural classes of the ISSS triangle (Fig. 2); (*ii*) the FAO and ISSS texture classes and the type of horizon (topsoil and subsoil horizons), to account for differences in pore structure, pore size, and OC content between the two horizons; (*iii*) the FAO and ISSS texture classes and bulk density, to account for the effect of soil structure on water retention; and (*iv*) the FAO texture classes, soil horizon, and bulk density in conjunction—this option was not available for the ISSS texture class-PTFs due to data limitations.

The class-PTFs were complemented by fitting the van Genuchten model (van Genuchten 1980) (Eqn 1) to the arithmetic mean value of θ at different water potentials using the RETC (retention curve) program (van Genuchten *et al.* 1991). The average water retention curves were obtained for the texture classes represented in the FAO and ISSS triangles after stratification by texture class, soil horizon (topsoil and subsoil), and bulk density as described above.

Uncertainty analyses

For each class-PTF type, the data were divided into two subsets: a calibration set composed of two-thirds of the data, and a validation set with the remaining one-third of the data. The random division and subsequent model development and validation were performed 10 times. Each time, the data that were used in the development of the class-PTFs were not used in validation, and *vice versa*. The class-PTFs were then established by averaging the arithmetic means of the water contents at each matric potential and the van Genuchten model parameters obtained in the 10 random development datasets. The standard deviations and the 95% confidence intervals for the means and standard deviations were also determined from the 10 random estimates. Class-PTFs having data from fewer than five horizons/layers were thus not considered due to the approach used here for analysing class-PTF uncertainty. In addition, it was assumed that estimates with fewer than five horizons would not produce a consistent estimate.

The precision bias and the average accuracy of the estimations were expressed by the mean error of predictions (MEP) and the RMSE, respectively, as follows:

$$\mathrm{MEP} = \frac{1}{H\,l}\sum_{j=1}^{H}\sum_{i=1}^{l}\left(\theta_{p,j,i} - \theta_{m,j,i}\right) \qquad (2)$$

$$\mathrm{RMSE} = \left\{\frac{1}{H\,l}\sum_{j=1}^{H}\sum_{i=1}^{l}\left(\theta_{p,j,i} - \theta_{m,j,i}\right)^2\right\}^{1/2} \qquad (3)$$

where $\theta_{p,j,i}$ is the predicted water content at potential i for horizon j; $\theta_{m,j,i}$ is the measured water content at potential i for horizon j; l is the number of water potentials for each horizon ($l = 10$ in this study); and H is the number of horizons ($H \leq 697$ in this study). The MEP and RMSE values were thus obtained for the estimates of volumetric water contents at each matric potential and not for the fitted van Genuchten model parameters, because the latter derived from the former. Positive and negative MEP values indicated overestimation and underestimation of the water contents, respectively. MEP and RMSE were determined for each of the 10 random validation datasets. The mean MEP

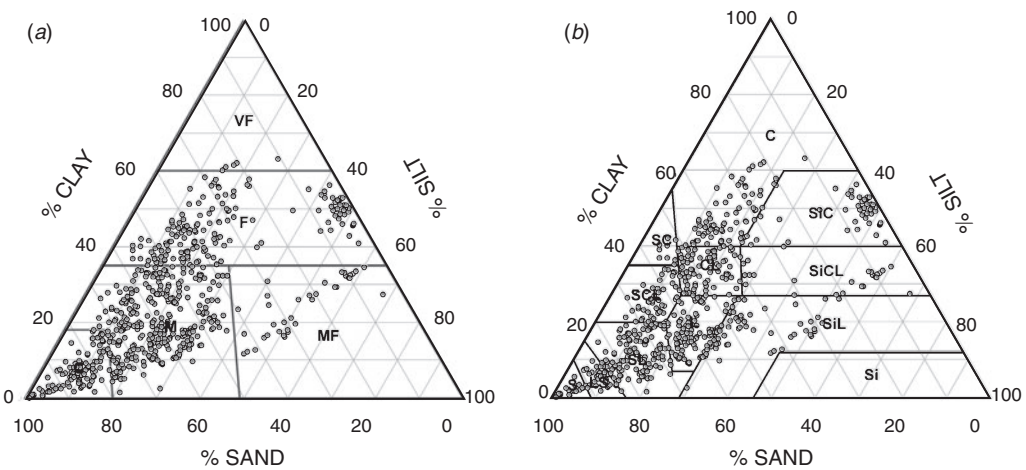

Fig. 2. Textural distribution of the 697 soil horizons classified in accordance with the (*a*) FAO and (*b*) ISSS textural classification systems. FAO triangle: C, coarse; M, medium; MF, medium fine; F, fine; VF, very fine texture classes. ISSS triangle: S, sand; LS, loamy sand; SL, sandy loam; L, loam; SCL, sandy clay loam; CL, clay loam; SC, sandy clay; C, clay; SiC, silty clay; SiCL, silty clay loam; SiL, silty loam; Si, silt.

and RMSE values, standard deviations, and 95% confidence intervals for the mean and standard deviation were also determined from the 10 estimates.

The accuracy of the class-PTFs was also compared with water content estimates from published PTFs that used part of our dataset (Gonçalves *et al.* 1997, 1999; Wösten *et al.* 1999; Paz *et al.* 2009). For the class and continuous PTFs of Wösten *et al.* (1999), it was necessary to interpolate the silt content, defined as the fraction between 2 and 50 µm, from the cumulative particle-size distribution of each horizon/layer included in our dataset. Smoothing splines (Nemes *et al.* 1999) were thus fitted to the cumulative particle size limits of 0, 2, 20, 200, and 2000 µm to obtain the cumulative percentage of particles at 50 µm. Smoothing splines were adjusted to the data with the Curve Fitting Toolbox 2.0 available in MATLAB R2009a version 7.8.0 (MathWorks Inc., Natick, MA, USA), resulting in an RMSE of 4.631%. However, because the most significant deviations were found for the fraction between 0 and 2 µm, the interpolation results for the fractions between 20 and 2000 µm and thus for the cumulative fraction at 50 µm were considered acceptable.

Assessment of the influence of the class-PTFs on the catchment water balance

A sensitivity analysis was performed using the river basin model SWAT (Soil and Water Assessment Tool; Neitsch *et al.* 2011) to assess the effect of different available water capacity (AWC) estimates on the catchment water balance. SWAT is a semi-distributed, process-oriented model for simulating water, nutrient, and pesticide transport. The hydrologic simulation is based on describing the water balance, which accounts for rainfall interception, evapotranspiration, surface runoff, infiltration, soil percolation, lateral flow, groundwater flow, and channel routeing processes.

In SWAT, surface runoff is computed using a modification of the SCS (Soil Conservation Services) curve number method (Neitsch *et al.* 2011). Reference evapotranspiration (ET_o) is calculated with the FAO Penman–Monteith method (Allen *et al.* 1998) and partitioned into soil evaporation and plant transpiration as described by Ritchie (1972). Soil percolation occurs when the field capacity of a soil layer is exceeded, and the percolation rate is governed by the *Ks* of the soil layer. Finally, lateral flow accounts for horizontal transport due to variations in the *Ks*, slope, and soil water content in the different sub-basins (Neitsch *et al.* 2011).

The sensitivity analysis was performed in the Enxoé catchment (60.8 km^2), in the Alentejo region of southern Portugal. The Enxoé is a tributary of the Guadiana River, one of the main rivers in the southern Iberian Peninsula. The dominant soils are Luvisols (covering 47% of the area), Cambisols (31%), Calcisols (14%), and Vertisols (6%) (FAO 1998). The main land uses are olive groves (18.3 km^2), agro-forestry of holm oak 'montado' (17.6 km^2), and annual winter crops (17.0 km^2). The agro-forestry of holm oak montado is mostly in areas with Cambisols, whereas olive groves and annual winter crops are mainly found in areas with Luvisols and Calcisols. The slopes are relatively gentle, and the average altitude of the catchment is 200 m.

Brito *et al.* (2012) studied the long-term dynamics of sediment and nutrients in that catchment using the SWAT model. Soil data were obtained from the European Soil Database version 2.0 (Daroussin *et al.* 2006), which comprises several specific databases, including the Soil Geographical Database of Eurasia (1 : 1 000 000) and the Soil Profile Analytical Database of Europa. The former is a simplified representation of the diversity and spatial variability of the soil coverage, whereas the latter incorporates quantitatively measured or estimated analytical data (e.g. texture, root depth, organic matter, and soil water retention) from representative soil profiles into soil mapping units. Although the soil data inputs were very generic, several parameters related to the travel time of water between the soil and the aquifer and between the aquifer and the river were calibrated and adjusted so that the SWAT estimates of the simulated flow regime were in good agreement with the field data. Further details can be found in Brito *et al.* (2012). The performance of the model was evaluated using the coefficient of efficiency (NSE) (Nash and Sutcliffe 1970):

$$\mathrm{NSE} = 1.0 - \frac{\sum_{i=1}^{N} (O_i - P_i)^2}{\sum_{i=1}^{N} (O_i - \overline{O})^2} \quad (4)$$

where N is the number of observations, O_i are the observations at time i, P_i is the model predictions at time i, and $\overline{O}$ is the average of observations; NSE = 1.0 represents a perfect fit, whereas negative NSE values indicate poor modelling performance.

The sensitivity analysis was performed by introducing different AWC estimates as inputs into the simulations of Brito *et al.* (2012). The AWC was here defined as the difference between the volumetric water contents at –33 and –1500 kPa matric potentials multiplied by the depth of the porous media. All other input parameters included in the simulations of Brito *et al.* (2012) were kept constant. The soil maps from Cardoso (1965), at a scale of 1 : 25.000, were used instead of the previous coarse-scale maps. The AWC was obtained by integrating each of the seven class-PTFs developed in this study into the regional soil maps. For each alternative estimate of AWC, the model performance was also evaluated using Eqn 4, and the different components of the catchment water balance determined using SWAT were compared.

Results and discussion

Performance analyses of the class-PTFs based on the FAO texture classification

The class-PTFs that were developed after grouping the data according to the different criteria are reported as follows. The class-PTFs following the five textural classes of the FAO triangle are presented in Table 2; and those following the FAO texture classes and bulk density are presented in Table 3. The resulting MEP and RMSE values obtained for each of these class-PTFs are presented in Table 4. Because of the amount of information obtained in the development of the class-PTFs, the standard deviations and the 95% confidence intervals

Table 2. Class pedotransfer functions established after stratification by FAO texture classes

N, Number of soil horizons; φ, total porosity; θ_i, volumetric water contents measured at –*i* kPa matric potentials

Class-PTF	*N*	φ	Volumetric water content									van Genuchten's parameters			
			$\theta_{0.25}$	θ_1	$\theta_{3.2}$	$\theta_{6.3}$	θ_{10}	θ_{33}	θ_{100}	θ_{250}	θ_{1500}	θ_r	θ_s	α	η
			(cm^3/cm^3)									(cm^3/cm^3)		(1/cm)	(–)
Very fine	5	0.541	0.528	0.504	0.479	0.465	0.457	0.428	0.391	0.364	0.318	0.052	0.535	0.103	1.082
Fine	162	0.496	0.484	0.463	0.440	0.422	0.410	0.373	0.333	0.306	0.260	0.039	0.488	0.059	1.103
Medium fine	36	0.529	0.516	0.495	0.474	0.461	0.451	0.407	0.331	0.281	0.197	0.032	0.508	0.009	1.213
Medium	386	0.421	0.401	0.376	0.348	0.328	0.314	0.269	0.222	0.192	0.142	0.039	0.406	0.041	1.197
Coarse	108	0.396	0.376	0.345	0.303	0.260	0.231	0.167	0.125	0.103	0.067	0.021	0.388	0.061	1.301

Table 3. Class pedotransfer functions established after stratification by FAO texture classes and dry bulk density (ρ_b)

N, Number of soil horizons; φ, total porosity; θ_i, volumetric water contents measured at –*i* kPa matric potentials

Class-PTF	*N*	φ	Volumetric water content									van Genuchten's parameters			
			$\theta_{0.25}$	θ_1	$\theta_{3.2}$	$\theta_{6.3}$	θ_{10}	θ_{33}	θ_{100}	θ_{250}	θ_{1500}	θ_r	θ_s	α	η
			(cm^3/cm^3)									(cm^3/cm^3)		(1/cm)	(–)
Very fine	–	–	–	–	–	–	–	–	–	–	–	–	–	–	–
Fine	162														
ρ_b <1.20	21	0.589	0.580	0.562	0.535	0.507	0.487	0.435	0.380	0.345	0.281	0.045	0.585	0.071	1.129
1.20≤ ρ_b <1.40	57	0.539	0.527	0.502	0.474	0.454	0.440	0.398	0.353	0.323	0.273	0.059	0.534	0.067	1.115
1.40≤ ρ_b <1.60	52	0.471	0.459	0.442	0.421	0.408	0.398	0.366	0.330	0.305	0.262	0.041	0.465	0.060	1.095
1.60≤ ρ_b	32	0.412	0.399	0.379	0.361	0.347	0.339	0.310	0.280	0.259	0.226	0.054	0.407	0.100	1.100
Medium fine	36														
ρ_b <1.20	11	0.583	0.570	0.547	0.516	0.496	0.484	0.422	0.331	0.276	0.184	0.031	0.562	0.012	1.242
1.20≤ ρ_b <1.40	19	0.537	0.523	0.503	0.483	0.470	0.461	0.419	0.347	0.301	0.218	0.072	0.515	0.009	1.237
1.40≤ ρ_b	6	0.394	0.388	0.367	0.354	0.347	0.343	0.314	0.250	0.200	0.138	0.039	0.376	0.006	1.276
Medium	386														
ρ_b <1.20	8	0.540	0.522	0.493	0.445	0.416	0.384	0.305	0.232	0.190	0.120	0.026	0.524	0.030	1.275
1.20≤ ρ_b <1.40	59	0.495	0.464	0.435	0.397	0.371	0.352	0.290	0.230	0.192	0.133	0.033	0.474	0.039	1.231
1.40≤ ρ_b <1.60	181	0.430	0.410	0.386	0.359	0.339	0.324	0.277	0.226	0.194	0.141	0.054	0.413	0.030	1.230
1.60≤ ρ_b <1.80	119	0.373	0.357	0.335	0.311	0.296	0.284	0.250	0.214	0.189	0.150	0.064	0.362	0.049	1.188
1.80≤ ρ_b	19	0.342	0.329	0.305	0.282	0.267	0.257	0.228	0.198	0.180	0.148	0.065	0.336	0.090	1.169
Coarse	108														
ρ_b <1.40	15	0.492	0.471	0.436	0.379	0.321	0.282	0.180	0.129	0.104	0.064	0.030	0.480	0.042	1.402
1.40≤ ρ_b <1.60	41	0.409	0.383	0.349	0.299	0.256	0.228	0.161	0.119	0.099	0.062	0.019	0.398	0.067	1.315
1.60≤ ρ_b <1.80	44	0.372	0.355	0.326	0.289	0.245	0.217	0.163	0.123	0.102	0.070	0.032	0.365	0.058	1.318
1.80≤ ρ_b	8	0.302	0.289	0.271	0.249	0.232	0.220	0.180	0.141	0.118	0.083	0.028	0.291	0.032	1.252

for the means and standard deviations cannot be presented here in detail.

The class-PTFs established for the FAO texture classes (Table 2) produced an acceptable estimation of φ and soil water retention when considering all texture classes combined (MEP = –0.001 cm^3/cm^3 with a 95% confidence interval of ±0.002 cm^3/cm^3). However, the water retention values in the medium fine texture classes were slightly overestimated, whereas they were slightly underestimated in the fine texture classes. Nevertheless, the RMSE values were relatively high, varying between 0.041 (±0.009) and 0.069 (±0.008) cm^3/cm^3 for the very fine and fine texture classes, respectively. Hence, the RMSE values obtained when combining all textures classes were also high (RMSE = 0.057 ± 0.001 cm^3/cm^3). The low accuracy of these class-PTFs was expected, because they resulted from an attempt to explain soil variability using only five average retention curves. The uncertainty related to these five average retention curves was mostly associated with volumetric water contents approaching to saturation, i.e. where the effect of pore size (macroporosity in particular) on water retention was more significant.

The class-PTFs established after the stratification by FAO texture classes and bulk density (Table 3) produced a significant improvement of the estimates of φ and soil water retention at different matric potentials. Table 3 shows that the effect of soil structure on the water retention curve was significant between φ and the –100 kPa matric potential, with soils with lower bulk density presenting higher water retention values and soils with higher bulk density values showing lower values for the water retention properties. The MEP for all texture classes combined was again good (MEP = 0.000 ± 0.001 cm^3/cm^3), and the estimates were more acceptable for each texture class individually, varying between –0.002 ± 0.004 and 0.002 ± 0.005 cm^3/cm^3 for the medium fine and coarse texture classes, respectively. The RMSE was 0.013 cm^3/cm^3 smaller for this class-PTF compared with that derived from texture class only. The performance of the class-PTF derived from the FAO texture classes and bulk density was better for the estimates produced for the medium fine and medium texture classes than for the fine texture class.

Inclusion of the type of horizon did not significantly improve the performance of the previous class-PTFs and thus they are not presented in detail. The RMSE values were only 0.001 cm^3/cm^3 smaller for these class-PTFs compared with those derived solely from texture class or when also considering bulk density (Table 4). Similar results were obtained by Al Majou *et al.* (2008*b*). A possible explanation is related to the size of the cores (100 cm^3) used to develop the class-PTFs. This small sample volume may have led to overestimations of the bulk density in tilled horizons/layers, with consequent underestimations of volumetric soil-water retention values. Thus, the possible effect of including the type of horizon was not reached, as soil

Table 4. Performance analyses of the class pedotransfer functions (class-PTFs) based on the FAO texture triangle, established after stratification by texture classes, soil horizon, and bulk density

N, Number of soil horizons used in validation

Class-PTF	*N*	Mean error of predictions, MEP (cm^3/cm^3)	Root mean square error, RMSE (cm^3/cm^3)
FAO texture classes			
Very fine	2	0.000	0.041
Fine	54	–0.004	0.069
Medium fine	12	0.006	0.062
Medium	129	–0.001	0.049
Coarse	36	0.002	0.059
All textures together	233	–0.001	0.057
FAO texture classes + soil horizon			
Very fine	–	–	–
Fine	55	0.000	0.067
Medium fine	13	0.001	0.061
Medium	129	0.003	0.049
Coarse	37	–0.004	0.056
All textures together	234	0.001	0.056
FAO texture classes + bulk density			
Very fine	–	–	–
Fine	54	0.002	0.052
Medium fine	13	–0.002	0.038
Medium	131	–0.001	0.038
Coarse	37	0.002	0.053
All textures together	235	0.000	0.044
FAO texture classes + soil horizon + bulk density			
Very fine	–	–	–
Fine	56	0.002	0.051
Medium fine	12	0.003	0.038
Medium	137	0.000	0.037
Coarse	38	0.001	0.051
All textures together	243	0.001	0.043

macroporosity was mostly not taken into account (Bruand *et al.* 2003). However, the constant sample volume used in all determinations (and generally standardised in many studies related to soil-water retention properties) allowed the comparison of different soils, land uses and managements, and laboratory methodologies. Other techniques, such as the clod bulk density, may be superior in those cases with tilled horizons because they may further include the structural (macroporosity) and textural porosity in tilled soils and their variability with time and management (Bruand *et al.* 2003).

The class-PTFs established according to the FAO texture classification and after stratification by texture classes, soil horizon, and bulk density produced RMSE values that varied between 0.043 and 0.057 cm^3/cm^3. These were comparable to most results available in the literature for evaluating the performance of different class-PTFs (e.g. Wösten *et al.* 2001; Schaap *et al.* 2001; Bruand *et al.* 2003; Al Majou *et al.* 2008*a*). Of particular note, only Al Majou *et al*. (2008*b*) were able to obtain smaller RMSE (0.013–0.050 cm^3/cm^3) than those of this study. Nevertheless, as the prediction accuracies depend on the extent of the area studied, on the spatial variability of soils within the area or database, and on the methods used for sampling and measurement (Wösten *et al.* 2001), the prediction accuracies found in the literature served here only as benchmarks.

Performance analyses of the class-PTFs based on ISSS texture classification

The class-PTFs based on the ISSS texture classification referred to (*i*) the 12 textural classes of the ISSS triangle, which are presented in Table 5; (*ii*) the ISSS texture classes and soil horizon, presented in Table 6; and (*iii*) the ISSS texture classes and bulk density, shown in Table 7. The resulting MEP and RMSE obtained for each of these class-PTFs are presented in Table 8. However, it was not possible to provide any estimate for the silt texture class, as the dataset contains no information for this texture (Fig. 2), and estimates for the sandy clay class were limited by the number of samples available.

The class-PTFs established for the ISSS texture classes (Table 5) produced an acceptable precision bias of the water retention estimates when considering all texture classes combined (MEP = 0.001 ± 0.002 cm^3/cm^3). However, the precision bias varied again slightly within each textural class, with water retention values in the clay loam texture class being underestimated and in the sandy clay texture class being overestimated. This latter relatively higher MEP value was obtained from only five soil horizons where the standard deviations (s.d.) of the water retention values in the different matric potentials were also high ($0.023 \leq$ s.d. ≤ 0.042). The clay loam and silty clay texture classes showed the highest uncertainty for the mean values of the water retention curve, with the 'true' values being associated with relatively large confidence intervals. The class-PTFs established for the ISSS texture classes also produced a large RMSE (0.052 ± 0.001 cm^3/cm^3) when considering all texture classes together, which may be comparable to the ones obtained for the class-PTFs based on FAO texture classification. Assuming 12 texture classes instead of five resulted in a decrease of the RMSE by 0.005 cm^3/cm^3. Thus, moving from the five texture classes of the FAO triangle to

Table 5. Class pedotransfer functions established after stratification by ISSS texture classes
N, Number of soil horizons; φ, total porosity; θ_i, volumetric water contents measured at $-i$ kPa matric potentials

Class-PTF	*N*	φ	Volumetric water content (cm^3/cm^3)								van Genuchten's parameters			
			$\theta_{0.25}$	θ_1	$\theta_{3.2}$	$\theta_{6.3}$	θ_{10}	θ_{33}	θ_{100}	θ_{250}	θ_{1500}	θ_r (cm^3/cm^3)	θ_s	α (1/cm)	η (–)
Sand	18	0.398	0.370	0.329	0.243	0.165	0.127	0.065	0.042	0.040	0.021	0.018	0.386	0.060	1.661
Loamy sand	38	0.404	0.386	0.356	0.323	0.272	0.236	0.159	0.115	0.091	0.055	0.022	0.394	0.039	1.378
Sandy loam	121	0.404	0.384	0.356	0.323	0.297	0.278	0.224	0.174	0.147	0.104	0.031	0.392	0.047	1.243
Sandy clay loam	51	0.398	0.384	0.363	0.338	0.321	0.309	0.279	0.245	0.224	0.187	0.063	0.393	0.086	1.137
Sandy clay	8	0.416	0.399	0.370	0.338	0.309	0.293	0.256	0.223	0.202	0.170	0.069	0.413	0.129	1.169
Clay	74	0.491	0.478	0.454	0.429	0.413	0.402	0.368	0.332	0.308	0.268	0.040	0.488	0.117	1.090
Clay loam	83	0.429	0.416	0.395	0.373	0.357	0.346	0.314	0.279	0.257	0.219	0.044	0.425	0.097	1.107
Loam	171	0.429	0.404	0.379	0.351	0.331	0.317	0.269	0.218	0.184	0.128	0.028	0.410	0.033	1.214
Silty loam	62	0.456	0.441	0.417	0.392	0.376	0.361	0.313	0.247	0.206	0.142	0.053	0.436	0.015	1.269
Silt	–	–	–	–	–	–	–	–	–	–	–	–	–	–	–
Silty clay loam	25	0.517	0.507	0.486	0.461	0.446	0.434	0.392	0.327	0.290	0.218	0.059	0.502	0.017	1.183
Silty clay	46	0.568	0.559	0.545	0.525	0.507	0.490	0.443	0.390	0.353	0.290	0.050	0.561	0.040	1.129

Table 6. Class pedotransfer functions established after stratification by ISSS texture classes and soil horizon (topsoil and subsoil)
N, Number of soil horizons; φ, total porosity; θ_i, volumetric water contents measured at –*i* kPa matric potentials

Class-PTF	*N*	φ	Volumetric water content									van Genuchten's parameters			
			$\theta_{0.25}$	θ_1	$\theta_{3.2}$	$\theta_{6.3}$	θ_{10}	θ_{33}	θ_{100}	θ_{250}	θ_{1500}	θ_r	θ_s	α	η
			(cm^3/cm^3)									(cm^3/cm^3)		(1/cm)	(–)
Topsoils	312														
Sand	6	0.439	0.415	0.371	0.275	0.204	0.164	0.076	0.052	0.049	0.026	0.023	0.427	0.053	1.673
Loamy sand	19	0.446	0.429	0.391	0.348	0.297	0.260	0.175	0.127	0.099	0.065	0.030	0.435	0.044	1.376
Sandy loam	65	0.402	0.383	0.352	0.321	0.295	0.277	0.223	0.177	0.152	0.109	0.044	0.389	0.047	1.255
Sandy clay loam	22	0.410	0.397	0.369	0.337	0.318	0.306	0.272	0.235	0.211	0.174	0.051	0.407	0.119	1.133
Sandy clay	–	–	–	–	–	–	–	–	–	–	–	–	–	–	–
Clay	37	0.505	0.492	0.463	0.431	0.411	0.398	0.360	0.323	0.300	0.258	0.056	0.504	0.145	1.104
Clay loam	33	0.461	0.448	0.420	0.389	0.369	0.355	0.315	0.277	0.253	0.215	0.043	0.459	0.127	1.118
Loam	85	0.444	0.413	0.384	0.352	0.330	0.315	0.266	0.215	0.179	0.120	0.014	0.422	0.040	1.209
Silty loam	24	0.452	0.437	0.413	0.386	0.366	0.349	0.300	0.231	0.192	0.130	0.031	0.435	0.020	1.247
Silt	–	–	–	–	–	–	–	–	–	–	–	–	–	–	–
Silty clay loam	7	0.507	0.495	0.476	0.450	0.432	0.419	0.373	0.312	0.274	0.205	0.055	0.493	0.028	1.188
Silty clay	14	0.574	0.564	0.547	0.524	0.498	0.479	0.422	0.364	0.328	0.265	0.056	0.570	0.036	1.143
Subsoils	377														
Sand	12	0.377	0.351	0.313	0.230	0.139	0.102	0.056	0.035	0.032	0.017	0.016	0.364	0.055	1.778
Loamy sand	19	0.370	0.351	0.329	0.300	0.251	0.213	0.140	0.098	0.077	0.044	0.018	0.359	0.034	1.415
Sandy loam	56	0.406	0.387	0.362	0.329	0.304	0.286	0.230	0.175	0.144	0.099	0.024	0.392	0.037	1.250
Sandy clay loam	29	0.387	0.372	0.356	0.337	0.323	0.311	0.283	0.250	0.232	0.194	0.068	0.379	0.063	1.131
Sandy clay	–	–	–	–	–	–	–	–	–	–	–	–	–	–	–
Clay	37	0.476	0.464	0.444	0.424	0.411	0.402	0.373	0.338	0.314	0.275	0.045	0.471	0.084	1.086
Clay loam	50	0.412	0.399	0.381	0.364	0.352	0.343	0.315	0.281	0.259	0.221	0.064	0.404	0.055	1.115
Loam	86	0.408	0.390	0.368	0.344	0.325	0.312	0.266	0.217	0.185	0.133	0.053	0.356	0.024	1.247
Silty loam	38	0.456	0.441	0.417	0.394	0.380	0.368	0.320	0.255	0.212	0.146	0.055	0.434	0.013	1.270
Silt	–	–	–	–	–	–	–	–	–	–	–	–	–	–	–
Silty clay loam	18	0.508	0.498	0.478	0.455	0.441	0.431	0.394	0.334	0.298	0.229	0.053	0.494	0.017	1.166
Silty clay	32	0.565	0.556	0.544	0.525	0.511	0.496	0.454	0.402	0.367	0.304	0.054	0.558	0.020	1.123

Table 7. Class pedotransfer functions established after stratification by ISSS texture classes and dry bulk density (ρ_b)

N, Number of soil horizons; φ, total porosity; θ_i, volumetric water contents measured at $-i$ kPa matric potentials

Class-PTF	*N*	φ	Volumetric water content									van Genuchten's parameters			
			$\theta_{0.25}$	θ_1	$\theta_{3.2}$	$\theta_{6.3}$	θ_{10}	θ_{33}	θ_{100}	θ_{250}	θ_{1500}	θ_r	θ_s	α	η
			(cm^3/cm^3)									(cm^3/cm^3)		(1/cm)	(–)
Sand	18														
ρ_b <1.60	10	0.421	0.392	0.352	0.258	0.198	0.162	0.076	0.052	0.049	0.026	0.018	0.409	0.065	1.586
1.60≤ ρ_b	8	0.374	0.350	0.309	0.226	0.121	0.082	0.050	0.029	0.026	0.015	0.014	0.360	0.050	1.906
Loamy sand	38														
ρ_b <1.40	10	0.494	0.474	0.437	0.381	0.321	0.280	0.186	0.127	0.097	0.059	0.052	0.482	0.042	1.404
1.40≤ ρ_b <1.60	12	0.411	0.390	0.361	0.327	0.263	0.224	0.144	0.107	0.085	0.051	0.028	0.399	0.039	1.437
1.60≤ ρ_b	16	0.352	0.337	0.312	0.292	0.253	0.219	0.154	0.110	0.091	0.057	0.025	0.342	0.030	1.372
Sandy loam	121														
ρ_b <1.40	21	0.502	0.480	0.448	0.403	0.368	0.343	0.272	0.207	0.171	0.112	0.018	0.488	0.043	1.247
1.40≤ ρ_b <1.60	43	0.421	0.399	0.369	0.338	0.312	0.295	0.235	0.177	0.148	0.101	0.026	0.405	0.038	1.254
1.60≤ ρ_b <1.80	45	0.365	0.348	0.322	0.292	0.270	0.253	0.208	0.167	0.141	0.104	0.023	0.356	0.061	1.208
1.80≤ ρ_b	12	0.322	0.309	0.281	0.256	0.240	0.230	0.192	0.154	0.132	0.099	0.035	0.313	0.054	1.219
Sandy clay loam	51														
ρ_b <1.60	21	0.432	0.416	0.389	0.360	0.341	0.329	0.293	0.256	0.233	0.195	0.059	0.427	0.111	1.135
1.60≤ ρ_b <1.80	25	0.373	0.359	0.344	0.322	0.308	0.296	0.269	0.237	0.219	0.183	0.060	0.367	0.072	1.130
1.80≤ ρ_b	5	0.350	0.342	0.325	0.304	0.289	0.276	0.249	0.223	0.202	0.166	0.055	0.346	0.075	1.144
Sandy clay	–	–	–	–	–	–	–	–	–	–	–	–	–	–	–
Clay	74														
ρ_b <1.20	5	0.564	0.548	0.507	0.451	0.420	0.406	0.371	0.328	0.309	0.266	0.104	0.567	0.262	1.129
1.20≤ ρ_b <1.40	27	0.523	0.508	0.477	0.447	0.425	0.412	0.376	0.338	0.313	0.273	0.063	0.521	0.164	1.100
1.40≤ ρ_b <1.60	32	0.469	0.459	0.439	0.419	0.405	0.395	0.362	0.327	0.302	0.260	0.030	0.464	0.070	1.091
1.60≤ ρ_b	10	0.436	0.427	0.408	0.392	0.382	0.375	0.346	0.314	0.294	0.258	0.055	0.431	0.068	1.090
Clay loam	83														
ρ_b <1.40	13	0.521	0.508	0.468	0.432	0.408	0.390	0.339	0.296	0.267	0.223	0.041	0.520	0.132	1.128
1.40≤ ρ_b <1.60	34	0.441	0.428	0.408	0.384	0.370	0.358	0.324	0.285	0.262	0.220	0.039	0.434	0.065	1.114
1.60≤ ρ_b <1.80	31	0.392	0.380	0.364	0.347	0.334	0.326	0.301	0.273	0.252	0.220	0.064	0.386	0.076	1.103
1.80≤ ρ_b	5	0.382	0.369	0.353	0.337	0.326	0.319	0.295	0.268	0.252	0.220	0.053	0.374	0.078	1.095
Loam	171														
ρ_b <1.40	29	0.494	0.455	0.423	0.382	0.357	0.342	0.283	0.226	0.186	0.124	0.021	0.468	0.045	1.225
1.40≤ ρ_b <1.60	95	0.434	0.409	0.386	0.359	0.339	0.324	0.274	0.220	0.185	0.124	0.024	0.413	0.027	1.224
1.60≤ ρ_b	47	0.370	0.355	0.330	0.308	0.292	0.280	0.244	0.206	0.177	0.134	0.057	0.356	0.035	1.220
Silty loam	62														
ρ_b <1.20	6	0.552	0.538	0.519	0.490	0.480	0.456	0.390	0.301	0.243	0.154	0.030	0.531	0.010	1.282
1.20≤ ρ_b <1.40	19	0.520	0.501	0.478	0.452	0.434	0.417	0.362	0.286	0.239	0.163	0.030	0.498	0.026	1.231
1.40≤ ρ_b <1.60	21	0.432	0.419	0.392	0.364	0.344	0.329	0.282	0.225	0.191	0.134	0.035	0.418	0.027	1.224
1.60≤ ρ_b	16	0.382	0.369	0.348	0.330	0.318	0.310	0.277	0.224	0.188	0.137	0.048	0.364	0.015	1.235
Silt	–	–	–	–	–	–	–	–	–	–	–	–	–	–	–
Silty clay loam	25														
ρ_b <1.20	7	0.600	0.588	0.564	0.530	0.507	0.493	0.428	0.330	0.278	0.182	0.021	0.580	0.013	1.238
1.20≤ ρ_b <1.40	10	0.534	0.523	0.502	0.480	0.466	0.457	0.420	0.361	0.323	0.248	0.047	0.518	0.017	1.155
1.40≤ ρ_b	8	0.403	0.392	0.375	0.354	0.343	0.331	0.304	0.272	0.250	0.212	0.070	0.397	0.061	1.122
Silty clay	46														
ρ_b <1.20	17	0.597	0.591	0.577	0.557	0.529	0.507	0.450	0.391	0.352	0.282	0.049	0.597	0.028	1.141
1.20≤ ρ_b <1.40	23	0.565	0.555	0.542	0.523	0.510	0.496	0.452	0.399	0.362	0.299	0.051	0.556	0.020	1.125
1.40≤ ρ_b	6	0.495	0.481	0.461	0.432	0.418	0.411	0.383	0.347	0.330	0.289	0.055	0.491	0.120	1.085

Table 8. Performance analyses of the class pedotransfer functions (class-PTFs) based on the ISSS texture triangle, established after stratification by texture classes, soil horizon, and bulk density

N, Number of soil horizons used in validation

Class-PTF	*N*	Mean error of predictions, MEP (cm^3/cm^3)	Root mean square error, RMSE (cm^3/cm^3)
ISSS texture classes			
Sand	6	0.003	0.054
Loamy sand	13	–0.001	0.055
Sandy loam	41	–0.003	0.053
Sandy clay loam	17	0.005	0.045
Sandy clay	3	0.009	0.103
Clay	25	0.001	0.049
Clay loam	28	–0.004	0.048
Loam	57	0.005	0.042
Silty loam	21	–0.002	0.064
Silt	–	–	–
Silty clay loam	9	0.011	0.068
Silty clay	16	0.000	0.047
All texture together	236	0.001	0.052
ISSS texture classes + soil horizon			
Sand	6	0.000	0.050
Loamy sand	14	0.001	0.046
Sandy loam	41	0.001	0.051
Sandy clay loam	18	0.002	0.043
Sandy clay	–	–	–
Clay	26	–0.002	0.049
Clay loam	28	–0.001	0.047
Loam	58	–0.003	0.040
Silty loam	21	–0.006	0.066
Silt	–	–	–
Silty clay loam	9	–0.002	0.067
Silty clay	16	0.002	0.049
All texture together	237	–0.001	0.049
ISSS texture classes + bulk density			
Sand	7	0.004	0.053
Loamy sand	14	0.004	0.043
Sandy loam	41	0.001	0.036
Sandy clay loam	18	0.001	0.040
Sandy clay	–	–	–
Clay	26	–0.004	0.046
Clay loam	30	0.002	0.039
Loam	58	0.000	0.032
Silty loam	22	0.005	0.044
Silt	–	–	–
Silty clay loam	10	–0.005	0.033
Silty clay	16	–0.001	0.042
All texture together	242	0.000	0.039

the 12 texture classes of the ISSS system did not result in a significant increase of the class-PTFs prediction accuracy. This was likely explained by the fact that the class-PTFs presented in this study also accounted for the variability in bulk density values, thus inducing part of the variability in the volumetric water contents. For this reason, Bruand *et al*. (2003) first estimated the water content on a mass basis, and only then multiplied it by the horizon bulk density. Those authors showed that the variability was much smaller when the gravimetric water contents were first predicted.

In contrast to the results obtained with the class-PTFs based on the FAO texture classification, the inclusion of soil horizon information in the class-PTFs based on the ISSS texture classes (Table 6) slightly improved the performance of these latter class-PTFs, with RMSE being 0.003 cm^3/cm^3 smaller.

Finally, the class-PTFs established after the stratification of the ISSS texture classes and bulk density (Table 7) produced the best estimates of φ and soil water retention at different matric potentials. Again, the inclusion of soil structure information through the bulk density had a significant effect on the performance of the class-PTFs. The precision bias of the water retention estimates when considering all texture classes combined was good (MEP = 0.000 ± 0.002 cm^3/cm^3; Table 8), although the water retention values were slightly underestimated in soils with silty clay loam texture and overestimated in soils with silty loam texture. The precision bias was thus worst for soils with medium textures. Gonçalves *et al*. (1997) had already faced similar difficulties in deriving continuous-PTFs for medium texture soils when using an early version of this dataset (230 soil horizons). The RMSE relative to all texture classes combined was the lowest obtained for all of the class-PTFs developed in this study (RMSE = 0.039 ± 0.001 cm^3/cm^3). The estimations for the loam soils were again the most accurate, whereas the results for sandy soils were worst.

Do we need new PTFs?

Table 9 presents the accuracy of published PTFs (Gonçalves *et al.* 1997, 1999; Wösten *et al.* 1999; Paz *et al.* 2009) that used a portion of our data. These PTFs were now tested on the entire dataset to evaluate their performance in predicting the hydraulic behaviour of the Portuguese soils. Most of them refer to parametric PTFs that describe the water retention properties as continuous curves using the van Genuchten model (Eqn 1), thus allowing the computation and comparison of water retention values at the corresponding matric potentials developed for the class-PTFs. The only exceptions were the point PTFs developed by Paz *et al*. (2009) for specific pressure heads, namely, for soil water retention at –0.25, –10, and –1500 kPa matric potentials.

Gonçalves *et al*. (1997) and Wösten *et al*. (1999) developed continuous PTFs for *all soils* (i.e. without grouping data) that resulted in similar RMSE values (0.044 and 0.045 cm^3/cm^3) when using various predictors instead of texture classes (Table 9). The errors found were thus comparable to the ones obtained for the class-PTFs based on the FAO texture classes (Table 4) and for most of the class-PTFs based on the ISSS texture classes (Table 8). The exception was the class-PTFs established after the stratification by ISSS texture classes and bulk density (Table 7), which resulted in a lower RMSE (0.039 cm^3/cm^3). Hence, these results show that estimates similar to, or even better than, those obtained by much more sophisticated functions could be achieved with the simpler PTFs presented. Nonetheless, the main advantage of the class-PTFs is the reduced number of basic predictors necessary to estimate the water retention properties of Portuguese soils. For a country where soil cartography shows so many constraints, as previously discussed, the number of predictors in a PTF is significant for those interested in mapping the water retention properties of soils.

Table 9. Accuracy of published pedotransfer functions in the estimation of water retention properties of soil horizons included in the dataset
RA, Regression analysis; GM, geometric means; Dataset, data used in the development of the PTFs; CS, coarse sand; FS, fine sand; $Si_{20\,\mu m}$, silt fraction at 20 μm; $Si_{50\,\mu m}$, silt fraction at 50 μm; C, clay; ρ_b, bulk density; Z, mean depth; OM, organic matter; depth, qualitative variable having the values 1 (topsoils) and 0 (subsoils); *N*, number of samples where the PTF could be applied; MEP, mean error of predictions; RMSE, root mean square error. Values in bold represent prediction accuracies of PTFs

Study	Published PTFs: Method	Published PTFs: Model	Dataset	Predictors	Accuracy of PTFs: Texture class	*N*	MEP	RMSE
1. Gonçalves *et al.* (1997)	RA, continuous PTFs	VG, m = 1	230	CS, FS, $Si_{20\,\mu m}$, C, ρ_b, Z, OM, pH	–	440	**–0.002**	**0.045**
2. Gonçalves *et al.* (1997)	RA, continuous PTFs	VG, m = 1	230	CS, FS, $Si_{20\,\mu m}$, C, ρ_b, Z, OM, pH	Fine	152	–0.008	0.050
					Medium	206	–0.002	0.048
					Coarse	82	–0.000	0.047
					All textures together	440	**–0.004**	**0.049**
3. Gonçalves *et al.* (1999)	RA, continuous PTFs	VG, m = 1 – 1/η	70	CS, FS, $Si_{20\,\mu m}$, C, ρ_b, OM, pH	–	440	**0.019**	**0.067**
4. Paz *et al.* (2009)	RA, point PTFs	–	304	CS, FS, $Si_{20\,\mu m}$, C, ρ_b, Z	–	697	**–0.018**	**0.128**
5. Wösten *et al.* (1999)	GM, class PTFs	VG, m = 1 – 1/η	54	FAO texture classes, depth	Very fine	5	0.043	0.062
					Fine	162	0.026	0.075
					Medium fine	17	–0.104	0.113
					Medium	421	0.014	0.057
					Coarse	92	–0.009	0.061
					All textures together	697	**0.011**	**0.064**
6. Wösten *et al.* (1999)	RA, continuous PTFs	VG, m = 1 – 1/η	54	$Si_{50\,\mu m}$, C, ρ_b, OM, depth	–	626	**–0.019**	**0.044**

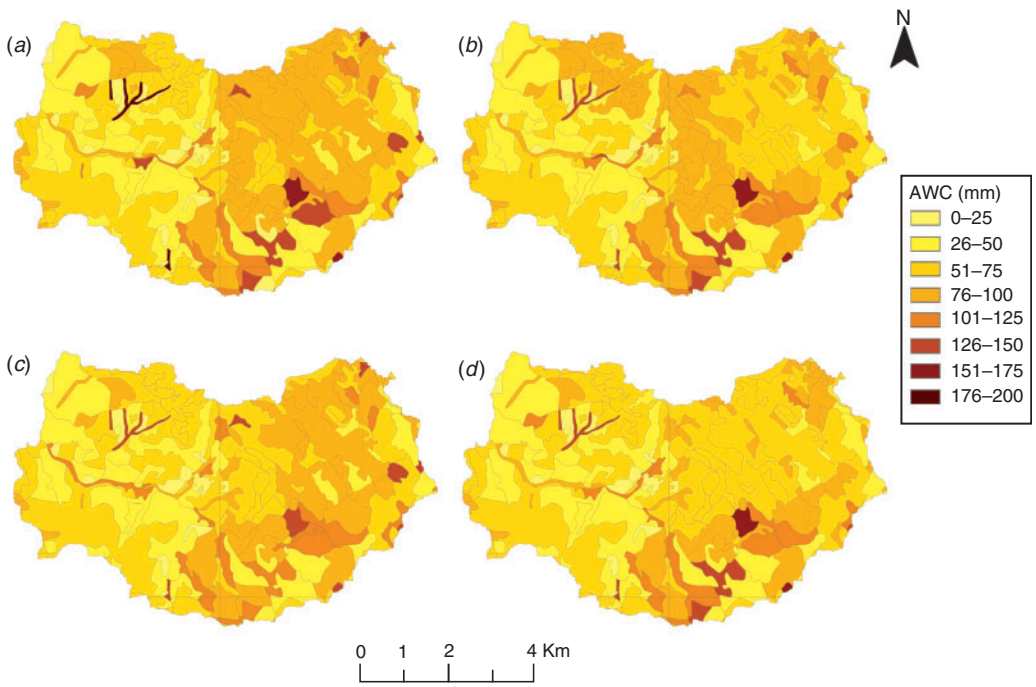

Fig. 3. Available water capacity (AWC) maps derived for the Enxoé catchment area by integrating the class-PTFs, established after grouping data by (*a*) FAO texture classes, (*b*) FAO textural classes and bulk density, (*c*) ISSS texture classes, (*d*) and ISSS texture classes and bulk density, into Portuguese soil maps at a scale of 1 : 25 000.

Wösten *et al.* (1999) also provided class-PTFs for European soils by grouping data by FAO texture classes and soil horizon. These resulted in RMSE = 0.064 cm^3/cm^3 when applied to our dataset (Table 9). Thus, the class-PTFs developed in this study, which used exactly the same inputs (Table 4), resulted in better estimates than the previous study. Curiously, the performance of

the PTFs developed using the HYPRES database (Wösten *et al.* 1999) in predicting the hydraulic behaviour of the Portuguese soils had not been previously assessed. Although the contribution from Portugal was only minor (54 soil horizons/layers; 104 samples with repetitions), the estimates of water retention properties can be considered adequate.

The literature on PTFs is abundant, and hydrological modellers may well find alternatives to the class-PTFs presented here (e.g. Schaap *et al.* 2001). However, the use of such 'external' PTFs causes two basic problems extensively discussed in the literature that should be first taken into account: (*i*) most 'external' or 'international' PTFs were never tested with Portuguese soil data, which means that the hydraulic characteristics of the Portuguese soils may fall outside the range of the original databases used to develop those PTFs (Wösten *et al.* 2001); and (*ii*) most PTFs were developed using different texture systems (normally the USDA texture system) from the one used in the Portuguese soil survey database (the ISSS system). Interpolation techniques are thus necessary to convert the ISSS texture limits into those required by 'international' PTFs (Nemes *et al.* 1999; Shirazi *et al.* 2001; Nemes and Rawls 2006). Users cannot simply start using PTFs regardless of their textural and regional validity.

Integrating soil hydraulic properties into soil mapping units

Figure 3 presents four different maps of the AWC for the Enxoé catchment. The maps were derived after integrating the class-PTFs into local soil maps (1 : 25 000) using the class-PTFs established according to the FAO texture classes (Fig. 3*a*), the FAO texture classes and bulk density (Fig. 3*b*), the ISSS texture classes (Fig. 3*c*), and the ISSS texture classes and bulk density (Fig. 3*d*).

The maps derived solely from soil texture classes (Fig. 3*a*, *c*) showed greater differences in AWC than the maps developed with both texture classes and bulk density (Fig. 3*b*, *d*). Differences among the four AWC maps were quite meaningful, namely in the eastern region of the catchment area where they approach 50 mm in some locations (Fig. 4).

The approach presented here is the simplest, most inexpensive, and most feasible technique available today to modellers for characterising soil hydraulic properties at large scales (Al Majou *et al.* 2008*b*), especially considering constraints such as those discussed above that are relevant to the Portuguese soil survey database. This approach was performed simply by grouping all of the available information on water retention properties of Portuguese soils in such a way that the derived maps were not validated *per se*. However, this information should facilitate soil characterisation for many of the applications being performed presently. No unique approach exists for upscaling soil hydraulic properties from soil cores to large catchment areas (Vogel and Roth 2003; Lin *et al.* 2006; Vereecken *et al.* 2007; Lin 2010). Most of these techniques are certainly more complex than the one presented here. Most of them also require more information on soil hydraulic properties than currently available for characterising catchment areas in Portugal, in particular those using geostatistical methods. One advantage of the approach followed here is that modellers can optimise the water retention

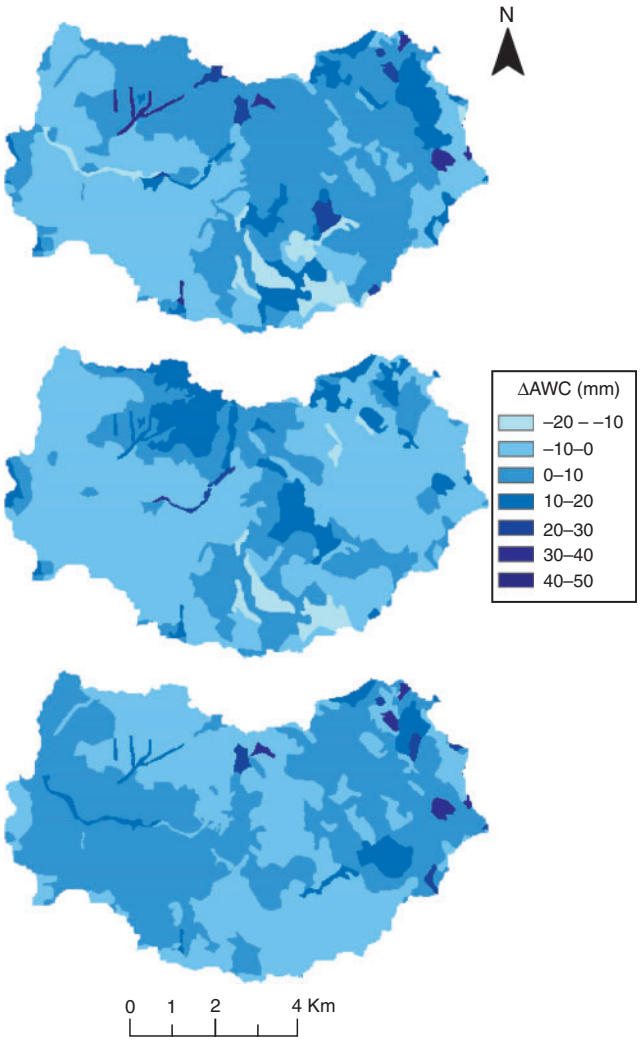

Fig. 4. Differences between the available water capacity (AWC) maps derived from the class-PTFs established after grouping data by FAO texture classes (top); FAO textural classes and bulk density (middle); ISSS texture classes (bottom) and the map derived from the class-PTFs established after the stratification of the ISSS texture classes and bulk density (reference map).

values of the catchment soils during parameter calibration, a common procedure in hydrological modelling for fitting measured and simulated discharges in the catchment area. However, modellers should be aware that going outside the confidence intervals of the considered class-PTFs would be ill advised.

Integration of class-PTFs into soil mapping units would ideally require minimal surveyed soil data (texture classes and bulk density) from the catchment area to better characterise soil hydraulic properties locally. Skilled pedologists can even determine soil texture classes manually. Hydrological modellers who do not possess such skills and cannot afford minimal soil survey studies should alternatively look for the required information in the representative soil profiles published in soil survey or PROPSOLO databases (Gonçalves *et al.* 2011). For bulk density, the latter database is the only option available. Particular attention should be given

Table 10. Water balance components of the Enxoé catchment estimated using the SWAT model based on different available water capacity inputs

Available water capacity inputs	Water balance components (%)				
	Runoff	Lateral flow	Evapotranspiration	Groundwater recharge	Deep aquifer loss
1. European Soil Database representative soil profiles	6.7	0.5	77.6	13.7	0.7
2. Class-PTFs					
FAO texture classes	5.6	2.1	73.2	17.6	0.9
FAO texture classes + soil horizon	5.6	1.8	73.3	17.9	0.9
FAO texture classes + bulk density	5.8	1.7	72.5	18.5	1.0
FAO texture classes + soil horizon+ bulk density	5.8	1.7	72.9	18.0	1.0
ISSS texture classes	5.9	1.6	73.2	17.4	0.9
ISSS texture classes + soil horizon	5.9	1.6	72.8	17.7	0.9
ISSS texture classes + bulk density	6.0	1.6	72.8	17.9	0.9

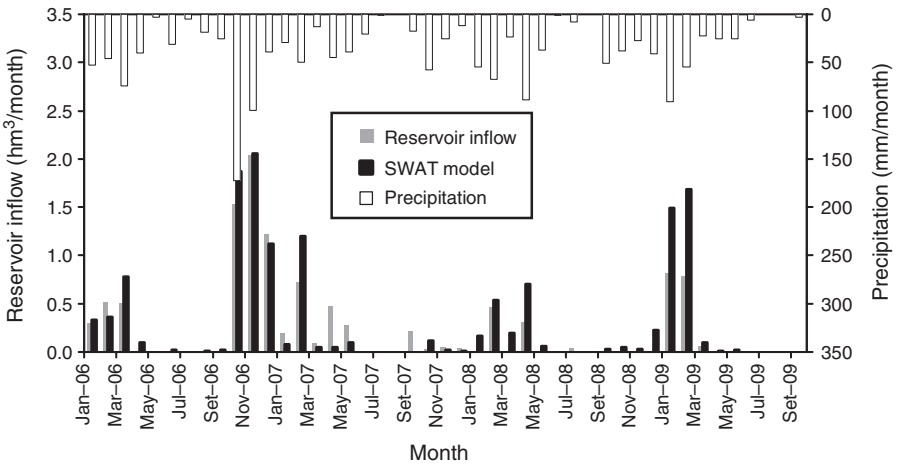

Fig. 5. Measured and simulated monthly inflows at the Enxoé reservoir.

to soil complexes, i.e. soil mapping units that include two or more soil units that cannot be represented separately at a specific scale on the soil map. For these complexes, Portuguese soil maps generally have the weighted distribution of each soil within the mapping unit. The quantification of map unit purity for different scales of soil maps is of fundamental importance for improving modern hydrological applications (Lin *et al.* 2006; Lin 2010). Therefore, that information should not be ignored. In Fig. 3, the AWC of soil complexes was in fact computed based on the weight of each soil unit within the soil-mapping unit. If information is available, the PTF with the smaller error should be used (Wösten *et al.* 2001; McBratney *et al.* 2002), this being the class-PTFs based on the ISSS texture classes and bulk density (Fig. 3*d*; Table 8).

Sensitivity analysis of a catchment model to different estimates of AWC

The SWAT model simulations of the catchment water balance using different AWC inputs are presented in Table 10. The information available in the European Soil Database and used in Brito *et al.* (2012) was estimated over large areas by expert judgement rather than measured on local soil samples. These estimations resulted from synthesis and generalisation of national or regional maps published at more detailed scales (Daroussin *et al.* 2006). Nevertheless, despite the use of generic, coarse-scale soil data, SWAT predicted reasonably well the monthly inflows of the catchment reservoir (NSE = 0.75), as shown by Brito *et al.* (2012).

The use of AWC soil maps at 1 : 25 000 derived from the class-PTFs as model inputs resulted in small differences compared with the results reported in Brito *et al.* (2012). The largest differences were found for the actual evapotranspiration, which decreased up to 4.6% when using the more detailed soil maps, whereas groundwater recharge increased up to 4.2% (Table 10). The small differences found were not particularly surprising, because the long-term results represent average annual behaviour (30-year simulation) and the difference in the level of detail of inputs is filtered in such a time scale. The fact that two datasets of distinct origins yield similar outputs confirms the results obtained in Enxoé.

A successful simulation of the reservoir inflow was obtained using all class-PTFs (Fig. 5; NSE >0.73). For long-term assessment (30-year water balance), the AWC soil maps at 1 : 25 000 derived from each of the class-PTFs successful estimated the water balance components of the Enxoé watershed. Moreover, these maps described soil spatial and vertical heterogeneity in more detail than the coarse-scaled

maps and are suited to implementations where the heterogeneity may be crucial for describing small-scale (space or time) processes (e.g. heavy rain concentrated in small areas producing localised runoff). Thus, although the use of AWC estimates based on different origins and levels of detail led to the equifinality problem (Ebel and Loague 2006; Bouma *et al.* 2011) in SWAT, i.e. different conditions led to the same effects, the use of more detailed soil maps complemented with the information provided by the class-PTFs contributed meaningfully to a better soil characterisation than that resulting from using coarse-scaled information.

The integration of the different class-PTFs into soil maps at 1 : 25 000 (Fig. 3) and their use as inputs to the SWAT model resulted in only small variations in the water balance components (Table 10). The largest variations were found for the actual evapotranspiration and groundwater recharge fractions, which varied only 0.8 and 1.1%, respectively. These small variations were somewhat expected because those maps also showed small variations in the AWC for most of the area (Fig. 4). Nonetheless, the class-PTF estimates may eventually be used as an inexpensive alternative to account for soil spatial variability in catchment areas.

Conclusions

The class-PTFs developed for Portuguese soils were established after stratifying data by texture classes, soil horizon, and bulk density. The accuracy of the predictions varied between 0.039 and 0.057 cm^3/cm^3. The best performances were obtained for the class-PTFs established after grouping the data by the 12 texture classes based on the ISSS particle limits and bulk density. The inclusion of the horizon type only slightly improved the prediction performance of the class-PTFs. The confidence intervals of the estimates were relatively narrow for most classes, with the exception of clay loam and silty clay texture classes.

Portuguese soil maps currently have many constraints to their use in modern hydrological studies. The class-PTFs developed here may partially overcome those constraints as they may be easily integrated into soil maps because only very basic soil data are required. For incorporating such information, minimal soil survey studies (texture classes and bulk density) need to be performed. For modellers without the necessary resources, the analysis of representative soil profiles included in soil survey or PROPSOLO databases would serve as an alternative. However, the use of those soil maps with different AWC estimates according to the integrated class-PTFs may only result in minimal differences when modelling the catchment water balance or other applications with a process-based, distributed hydrological model such as SWAT, which is less sensitive to the soil hydraulic properties. Nonetheless, those inputs may contribute to a better soil characterisation than when using coarse-scaled information.

The approach presented here gathered all of the currently available knowledge on soil hydraulic properties of Portuguese soils. This approach is the simplest, cheapest, and most feasible technique available today to modellers without many resources for characterising water retention properties at large scales.

Acknowledgements

This research was performed within the framework of the Project PTDC/AGR-AAM/098100/2008 of the Fundação para a Ciência e a Tecnologia (FCT). T. B. Ramos was funded by the FCT grant SFRH/BD/60363/2009.

References

Al Majou H, Bruand A, Duval O, Le Bas C (2008*a*) The use of in situ volumetric water content at field capacity to improve the predictions of soil water retention properties. *Canadian Journal of Soil Science* **88**, 533–541. doi:10.4141/CJSS07065

Al Majou H, Bruand A, Duval O, Le Bas C, Vautier A (2008*b*) Prediction of soil water retention properties after stratification by combining texture, bulk density and the type of horizon. *Soil Use and Management* **24**, 383–391. doi:10.1111/j.1475-2743.2008.00180.x

Allen RG, Pereira LS, Raes D, Smith M (1998) 'Crop evapotranspiration—Guidelines for computing crop water requirements.' Irrigation and Drainage Paper No. 56. (FAO: Rome)

Baker L (2008) Development of class pedotransfer functions of soil water retention—A refinement. *Geoderma* **144**, 225–230. doi:10.1016/j.geoderma.2007.11.017

Bouma J (1989) Using soil survey data for quantitative land evaluation. *Advances in Soil Science* **9**, 177–213. doi:10.1007/978-1-4612-3532-3_4

Bouma J (2006) Hydropedology as a powerful tool for environmental policy research. *Geoderma* **131**, 275–286. doi:10.1016/j.geoderma.2005.03.009

Bouma J, Droogers P, Sonneveld MPW, Ritsema CJ, Hunink JE, Immerzeel WW, Kauffman S (2011) Hydropedological insights when considering catchment classification. *Hydrology and Earth System Sciences* **15**, 1909–1919. doi:10.5194/hess-15-1909-2011

Brito D, Neves R, Branco MA, Prazeres Â, Rodrigues S, Gonçalves MC, Ramos TB (2012) Assessing the long-term dynamics and nutrient loads to an eutrophic reservoir in a temporary river in southeast Portugal (Enxoé). *Journal of Hydrology*, in press.

Bruand A, Pérez Fernandez P, Duval O (2003) Use of class pedotransfer functions based on texture and bulk density of clods to generate water retention curves. *Soil Use and Management* **19**, 232–242. doi:10.1111/j.1475-2743.2003.tb00309.x

Cardoso JC (1965) 'Os Solos de Portugal. Sua classificação, caracterização e génese. I—A sul do Rio Tejo.' (Direcção Geral dos Serviços Agrícolas: Lisboa)

Dane JH, Hopmans JW (2002) Pressure plate extractor. In 'Methods of soil analysis, Part 4. Physical methods'. (Eds JH Dane, GC Topp) pp. 688–690. (Soil Science Society of America: Madison, WI)

Dane JH, Topp GC (2002) 'Methods of soil analysis. Part 4. Physical methods.' (Soil Science Society of America: Madison, WI)

Daroussin J, King D, Le Bas C, Vrščaj B, Dobos E, Montanarella L (2006) The Soil Geographical Database of Eurasia at Scale 1 : 1.000.000: history and perspective in digital soil mapping. *Developments in Soil Science* **31**, 55–65. doi:10.1016/S0166-2481(06)31004-5

Duarte P, Azevedo B, Guerreiro M, Ribeiro C, Bandeira R, Pereira A, Falcão M, Serpa D, Reia J (2008) Biochemical modelling of Ria Formosa (South Portugal). *Hydrobiologia* **611**, 115–132. doi:10.1007/s10750-008-9464-3

Ebel BA, Loague K (2006) Physics-based hydrologic-response simulation: Seeing through the fog of equifinality. *Hydrological Processes* **20**, 2887–2900. doi:10.1002/hyp.6388

FAO (1998) 'World reference base for soil resources.' World Soil Resources Report No. 84. (FAO: Rome)

Gomes MP, Silva AA (1962) Um novo diagrama triangular para a classificação básica da textura do solo. *Garcia da Orta* **10**, 171–179.

Gomes MP, Silva AA (1980). Inserção das grandes divisões e subdivisões da textura do solo adoptadas pela FAO (1970) no diagrama de classificação de Gomes & Silva (1962). In 'Congresso 80 da Ordem dos Engenheiros'. Coimbra. (Ordem dos Engenheiros: Lisbon)

Gonçalves MC, Pereira LS, Leij FJ (1997) Pedo-transfer functions for estimating unsaturated hydraulic properties of Portuguese soils. *European Journal of Soil Science* **48**, 387–400. doi:10.1046/j.1365-2389.1997.00095.x

Gonçalves MC, Almeida VV, Pereira LS (1999) Estimation of hydraulic parameters for Portuguese soils. In 'Characterization and measurement of the hydraulic properties of unsaturated porous media. Part 2'. (Eds MTh van Genuchten, F Leij, L Wu) pp. 1199–1210. (University of California: Riverside, CA)

Gonçalves MC, Reis LCL, Pereira MV (2005) Progress of soil survey in Portugal. In 'European Soil Bureau Research Report No. 9'. (Eds RJA Jones, B Houšková, P Bullock, L Montanarella) pp. 275–279. (Office for Official Publications of the European Communities: Luxembourg)

Gonçalves MC, Ramos TB, Pires FP (2011) Base de dados georreferenciada das propriedades do solo. In 'Agrorrural. Contributos Científicos'. (Eds PS Coelho, P Reis) pp. 564–574. (Instituto Nacional dos Recursos Biológicos: Oeiras, Portugal)

Jana RB, Mohanty BP (2012) A comparative study of multiple approaches to soil hydraulic parameter scaling applied at the hillslope scale. *Water Resources Research* **48**, W02520. doi:10.1029/2010WR010185

Lin H (2003) Hydropedology: bridging disciplines, scales, and data. *Vadose Zone Journal* **2**, 1–11.

Lin H (2010) Earth's Critical Zone and hydropedology: concepts, characteristics, and advances. *Hydrology and Earth System Sciences* **14**, 25–45. doi:10.5194/hess-14-25-2010

Lin H, Bouma J, Pachepsky Y, Western A, Thompson J, van Genuchten MTh, Vogel H-J, Lilly A (2006) Hydropedology: Synergistic integration of pedology and hydrology. *Water Resources Research* **42**, W05301. doi:10.1029/2005WR004085

Madeira M, Constantino AT, Réffega AG, Martins AA, Alexandre CJ, Sousa E, Monteiro FG, Pinheiro JF, Cardoso JC, Silva JV, Ricardo RP (2004) 'Bases para a revisão e actualização da classificação dos solos de Portugal.' (Sociedade Portuguesa de Ciência do Solo: Lisbon)

McBratney AB, Minasny B, Cattle SR, Vervoort RW (2002) From pedotransfer functions to soil inference systems. *Geoderma* **109**, 41–73. doi:10.1016/S0016-7061(02)00139-8

Nash JE, Sutcliffe JV (1970) River flow forecasting through conceptual models. I. A discussion of principles. *Journal of Hydrology* **10**, 282–290. doi:10.1016/0022-1694(70)90255-6

Neitsch SL, Arnold JG, Kiniry JR, Williams JR (2011) Soil and Water Assessment Tool, Theoretical documentation, version 2009. Texas Water Resources Institute Technical Report No. 406. (Texas A&M University System: College Station, TX)

Nelson DW, Sommers LE (1982) Total carbon, organic carbon, and organic matter. In 'Methods of soil analysis. Part 2. Chemical and microbiological properties'. (Eds AL Page, *et al.*) pp. 539–579. (ASA and SSSA: Madison, WI)

Nemes A, Rawls WJ (2006) Evaluation of different representations of the particle-size distribution to predict soil water retention. *Geoderma* **132**, 47–58. doi:10.1016/j.geoderma.2005.04.018

Nemes A, Wösten JHM, Lilly A, Oude Voshaar JH (1999) Evaluation of different procedures to interpolate particle-size distribution to achieve compatibility within soil databases. *Geoderma* **90**, 187–202. doi:10.1016/S0016-7061(99)00014-2

Nemes A, Schaap MG, Wösten JHM (2003) Functional evaluation of pedotransfer functions derived from different scales of data collection. *Soil Science Society of America Journal* **67**, 1093–1102. doi:10.2136/sssaj2003.1093

Nunes JP, Lima JLMP, Singh VP, Lima MIP, Vieira GN (2006) Numerical modeling of surface runoff and erosion due to moving rainstorms at the drainage basin scale. *Journal of Hydrology* **330**, 709–720. doi:10.1016/j.jhydrol.2006.04.037

Pachepsky YA, Rawls WJ (2004) 'Development of pedotransfer functions in soil hydrology.' (Elsevier: Amsterdam)

Pachepsky YA, Rawls WJ, Lin HS (2006) Hydropedology and pedotransfer functions. *Geoderma* **131**, 308–316. doi:10.1016/j.geoderma.2005.03.012

Paz AM, Cipriano D, Gonçalves MC, Pereira LS (2009) Funções de pedotransferência para a curva de retenção da água no solo. *Revista de Ciências Agrárias* **32**, 337–343.

Ritchie JT (1972) Model for predicting evaporation from a row crop with incomplete cover. *Water Resources Research* **8**, 1204–1213. doi:10.1029/WR008i005p01204

Romano N, Hopmans JW, Dane JH (2002) Suction table. In 'Methods of soil analysis, Part 4. Physical methods'. SSSA Book Series. (Eds JH Dane, GC Topp) pp. 692–698. (Soil Science Society of America: Madison, WI)

Schaap MG, Leij FJ, van Genuchten MTh (2001) ROSETTA: a computer program for estimating soil hydraulic parameters with hierarchical pedotransfer functions. *Journal of Hydrology* **251**, 163–176. doi:10.1016/S0022-1694(01)00466-8

Shirazi MA, Boersma L, Johnson CB (2001) Particle-size distributions: comparing texture systems, adding rock and predicting soil properties. *Soil Science Society of America Journal* **65**, 300–310. doi:10.2136/sssaj2001.652300x

Steenpass C, Vanderborght J, Herbst M, Šimůnek J, Vereecken H (2010) Estimating soil hydraulic properties from infrared measurements of soil surface temperatures and TDR data. *Vadose Zone Journal* **9**, 910–924. doi:10.2136/vzj2009.0176

van Genuchten MTh (1980) A closed form equation for predicting the hydraulic conductivity of unsaturated soils. *Soil Science Society of America Journal* **44**, 892–898. doi:10.2136/sssaj1980.03615995004400050002x

van Genuchten MTh, Leij FJ, Yates SR (1991) 'The RETC code for quantifying the hydraulic functions of unsaturated soils.' (U.S. Environmental Protection Agency: Ada, OK)

Vereecken H, Maes J, Feyen J, Darius P (1989) Estimating the soil moisture retention characteristics from texture, bulk density, and carbon content. *Soil Science* **148**, 389–403. doi:10.1097/00010694-198912000-00001

Vereecken H, Kasteel R, Vanderborght J, Harter T (2007) Upscaling hydraulic properties and soil water flow processes in heterogeneous soils: a review. *Vadose Zone Journal* **6**, 1–28. doi:10.2136/vzj2006.0055

Vogel HJ, Roth K (2003) Moving through scales of flow and transport in soil. *Journal of Hydrology* **272**, 95–106. doi:10.1016/S0022-1694(02)00257-3

Weihermüller L, Huisman JA, Lambot S, Herbst M, Vereecken H (2007) Mapping the spatial variation of soil water content at the field scale with different ground penetrating radar techniques. *Journal of Hydrology* **340**, 205–216. doi:10.1016/j.jhydrol.2007.04.013

Wösten JHM, Finke PA, Jansen MJW (1995) Comparison of class and continuous pedotransfer functions to generate soil hydraulic characteristics. *Geoderma* **66**, 227–237. doi:10.1016/0016-7061(94)00079-P

Wösten JHM, Lilly A, Nemes A, Le Bas C (1999) Development and use of a database of hydraulic properties of European soils. *Geoderma* **90**, 169–185. doi:10.1016/S0016-7061(98)00132-3

Wösten JHM, Pachepsky YA, Rawls WJ (2001) Pedotransfer functions: bridging the gap between available basic soil data and missing soil hydraulic characteristics. *Journal of Hydrology* **251**, 123–150. doi:10.1016/S0022-1694(01)00464-4

Yevenes MA, Mannaerts CM (2011) Seasonal and land use impacts on the nitrate budget and export of a mesoscale catchment in Southern Portugal. *Agricultural Water Management* **102**, 54–65. doi:10.1016/j.agwat.2011.10.006